



Aalborg Universitet

AALBORG UNIVERSITY
DENMARK

Resonance Damping Techniques for Grid-Connected Voltage Source Converters with LCL filters – A Review

Zhang, Chi; Dragicevic, Tomislav; Vasquez, Juan Carlos; Guerrero, Josep M.

Published in:

Proceedings of the 2014 IEEE International Energy Conference (ENERGYCON)

DOI (link to publication from Publisher):

[10.1109/ENERGYCON.2014.6850424](https://doi.org/10.1109/ENERGYCON.2014.6850424)

Publication date:

2014

Document Version

Early version, also known as pre-print

[Link to publication from Aalborg University](#)

Citation for published version (APA):

Zhang, C., Dragicevic, T., Vasquez, J. C., & Guerrero, J. M. (2014). Resonance Damping Techniques for Grid-Connected Voltage Source Converters with LCL filters – A Review. In *Proceedings of the 2014 IEEE International Energy Conference (ENERGYCON)* (pp. 169-176). IEEE Press. I E E E International Energy Conference. ENERGYCON proceedings <https://doi.org/10.1109/ENERGYCON.2014.6850424>

General rights

Copyright and moral rights for the publications made accessible in the public portal are retained by the authors and/or other copyright owners and it is a condition of accessing publications that users recognise and abide by the legal requirements associated with these rights.

- Users may download and print one copy of any publication from the public portal for the purpose of private study or research.
- You may not further distribute the material or use it for any profit-making activity or commercial gain
- You may freely distribute the URL identifying the publication in the public portal -

Take down policy

If you believe that this document breaches copyright please contact us at vbn@aub.aau.dk providing details, and we will remove access to the work immediately and investigate your claim.

Resonance Damping Techniques for Grid-Connected Voltage Source Converters with *LCL* filters – A Review

Chi Zhang, Tomislav Dragicevic, Juan C. Vasquez and Josep M. Guerrero

Microgrids Research Programme www.microgrids.et.aau.dk

Department of Energy, Aalborg University, Pontoppidanstraede 101, 9220 Aalborg, Denmark

{zhc, tdr, juq, joz}@et.aau.dk

Abstract—*LCL* filters play an important role in grid-connected converters when trying to reduce switching-frequency ripple currents injected into the grid. Besides, their small size and low cost make them attractive for many practical applications. However, the *LCL* filter is a third-order system, which presents a resonance peak frequency. Oscillation will occur in the control loop in high frequency ranges, especially in current loop in double-loops controlled converters. In order to solve this, many strategies have been proposed to damp resonance, including passive and active methods. This paper makes a review of these methods.

Keywords: *LCL* filter, Active damp methods, Passive damp methods, Grid-connected inverter

I. INTRODUCTION

Nowadays voltage source converters (VSC) have become an essential part of many sources and appliances when connecting to the grid. Traditionally voltage source converters are connected to the grid by means of a single inductor (L), in order to reduce the switching frequency ripple currents. However, more and more inductor-capacitor-inductor (*LCL*) filters are becoming popular due to their performance in attenuating harmonics and fast dynamic response. Moreover, their small size and low cost are also attractive for application engineers.

In [1] and [5], detailed design procedures of *LCL* filter were presented. According to the requirements of current ripple tolerance, voltage drop, resonance frequency, reactive power rate, and losses, *LCL* filter parameters can be designed, including converter side inductor (L), capacitor (C) and grid side inductor (L_g).

VSC with *LCL* filters are more sensitive to grid distortion, which needs for more advanced control strategies in order to maintain better stability performance [2]. So that many passive and active methods were proposed in order to satisfy system stability requirements.

In order to suppress *LCL* filters resonance, passive methods [3]-[8] are easier and cheaper for stiff-grid applications [3]. However, it may produce extra losses and may affect high-frequency harmonic attenuation capability.

The basic types of passive damping methods are presented in [4] and [16]. Passive elements like resistors, inductors, and capacitors are placed using different combinations. However, it is really challenging to trade-off losses and filter performance.

In order to solve this problem, active damping methods are gaining more attention ([2], [9]-[21]). With the aim to eliminate the extra losses produced by passive damping process, a virtual resistor is proposed in order to mimic a real damping resistor by using an additional control loop in [12]-[13]. However, the resonance peak still persists in the control loop, and consequently two current feedback control strategies are proposed in [2] and [9]. By using a "weighted current feedback" approach, these two strategies aim at modifying the transfer function of *LCL* filter in closed-loop towards single inductor filter behaviour, being inherently stable. However the control design depends on *LCL* physical parameters.

In [10], [14] and [15], a lead-lag compensator is added into the current loop, being effective inside a small range around the resonance frequency, while no interference is introduced in both low frequency and switching frequency. In [17], different feedback loops were investigated to evaluate their performance. Based on these basic damping methods, several improved damping techniques are proposed in [18]-[21]. Hybrid damping methods [18] combine passive with active ones together to overcome drawbacks, while a grid current feedback damping strategy aiming at reducing current sensor's number is presented in [20]. Further, genetic algorithm (GA) is adopted in [19] to adapt an active damping method to different conditions in case of *LCL* physical parameters' mismatch. Considering microgrids applications, a method including two impedance feedback loops is proposed in [21].

This paper presents a review which encompasses different damping methods adopted in grid-connected voltage source converters. Section II presents the basic concepts of *LCL* filters in parallel inverters forming microgrids. Then different methods, including passive, active methods and other improved ones, are reviewed in Section III and Section IV. Finally, conclusion is presented in Section V.

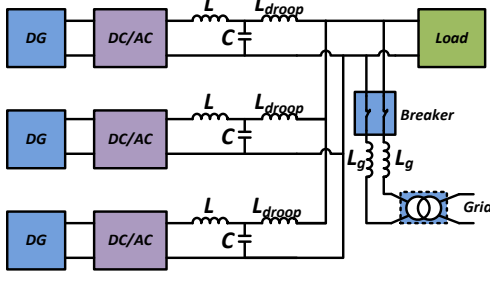


Fig. 1. Microgrid power stage structure.

II. LCL FILTER IN PARALLEL INVERTERS FORMING MICROGRIDS

In distribution generation systems, several DC/AC work as voltage sources to form a MicroGrid which often use droop control [22]-[23]. In Fig. 1, basic structure is shown. An LC filter is connected to each DC/AC output and L_{droop} acts as a droop inductor. Usually one inverter is operating as a voltage source, while the others adopt a current control strategy. Here L , C , and L_{droop} can be seen as an LCL filter in grid-connected mode, so that interactions between LCL filters and the grid will occur and may affect the system performance. With a better comprehension about LCL filters, especially in parallel system, interactions can be suppressed successfully, which will endow a robust performance to the system.

III. PASSIVE DAMPING METHODS

Passive methods win much attention because of its simplicity, cost effective, and simple implementation. It mainly deals with LCL filter hardware circuit itself. As shown in Fig. 2, resistors, inductors and capacitors are the three main elements in passive damping methods. Sub-circuits, with a combination of these three elements, are inserted into LCL filters to damp its resonance. Consequently, more poles and zeroes may appear (see (1)) to cancel inherent poles in LCL filter transfer function.

In Fig. 3, several basic kinds of passive damping methods are shown. By using different damping strategies, LCL filters will have different performance in both low and high frequency ranges. It can be seen from Fig. 4 that passive damping methods target to eliminate the resonance peak while sacrificing filter performance. In Fig. 3, the simplest configuration is *circuit a*, which reduce resonance peak by inserting a resistor into the C 's branches. In order to obtain a better trade-off between performance and resistive losses reduction [5], more devices (inductors and capacitors) are added as a damping sub-circuit (see Fig.3). However, with these solutions raise the cost and complexity of the filter. Further, although resonance peak is well dealt with, performance in high-frequency range is degraded at the same time. Note that the slope of the Bode diagram in high frequency range is smaller than the LCL filter open-loop one, resulting in a poorer performance. Taking *circuit c* (see Fig. 3) as an example, it introduces another resonance peak (see Fig.4)

while bringing LCL filter resonance peak down at the expense of increasing filter complexity. So that a trade-off between filtering and damping performances should be taken into account. In addition, when designing passive damping aid circuits, extra losses that will affect converter's efficiency should be also taken into account. Moreover, nonlinearities in devices, such as inductors and capacitors, may cause serious EMI and/or EMC problems.



Fig. 2. Main elements used in passive damping techniques.

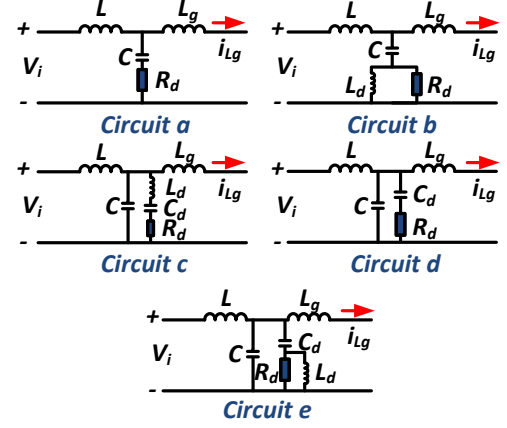


Fig. 3. Passive damping methods.

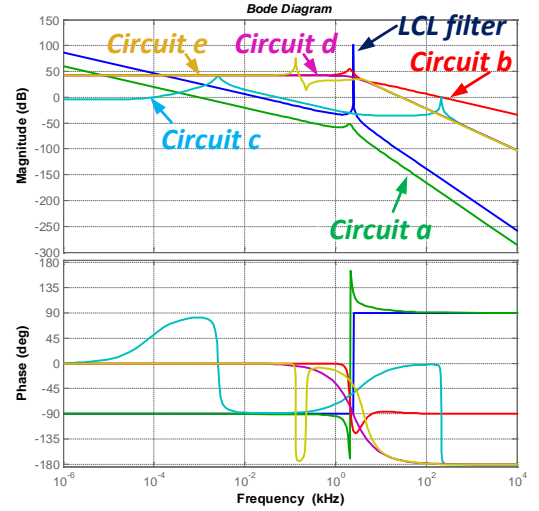


Fig. 4. Bode diagram of different damping circuits.

IV. ACTIVE DAMPING METHODS

Compared to the passive damping methods, active damping techniques are mainly focused on control strategies. By adding additional damping control loops, especially in current loops, negative effects caused by LCL filter can be minimized to a large extent.

$$\begin{aligned}
G(s) &= \frac{i_{L_g}}{V_i} = \frac{1}{LL_g Cs^3 + (L + L_g)s} \quad (\text{Original Transfer Function of LCL Filter}) \\
G(s) &= \frac{i_{L_g}}{V_i} = \frac{R_d Cs + 1}{LL_g Cs^3 + (L + L_g)R_d Cs^2 + (L + L_g)s} \quad (\text{Circuit a}) \\
G(s) &= \frac{i_{L_g}}{V_i} = \frac{L_d R_d Cs^2 + L_d s + R_d}{LL_g L_d Cs^4 + (LL_g + LL_d + L_g L_d)R_d Cs^3 + (L + L_g)L_d s^2 + (L + L_g)R_d s} \quad (\text{Circuit b}) \\
G(s) &= \frac{i_{L_g}}{V_i} = \frac{L_d C_d s^2 + R_d C_d s + L_g}{LL_g L_d C_d Cs^5 + LL_g R_d C_d Cs^4 + (LL_g C_d + LL_g C + LC_d R_d + L_g L_d C_d)s^3 + (LR_d C_d + L_g R_d C_d)s^2 + (L + L_g)s} \quad (\text{Circuit c}) \\
G(s) &= \frac{i_{L_g}}{V_i} = \frac{R_d C_d s + 1}{LL_g R_d C_d Cs^4 + LL_g C_d s^3 + LL_g Cs^3 + (L + L_g)R_d C_d s^2 + (L + L_g)s} \quad (\text{Circuit d}) \\
G(s) &= \frac{i_{L_g}}{V_i} = \frac{L_d R_d C_d s^2 + L_d s + R_d}{LL_d L_g R_d C_d Cs^5 + LL_d L_g C_d s^4 + LL_d L_d Cs^4 + LL_g R_d C_d s^3 + LL_d R_d C_d s^3 + LL_g R_d Cs^3 + L_g L_d R_d C_d s^3 + (L + L_g)L_d s^2 + (L + L_g)R_d s} \quad (\text{Circuit e})
\end{aligned} \tag{1}$$

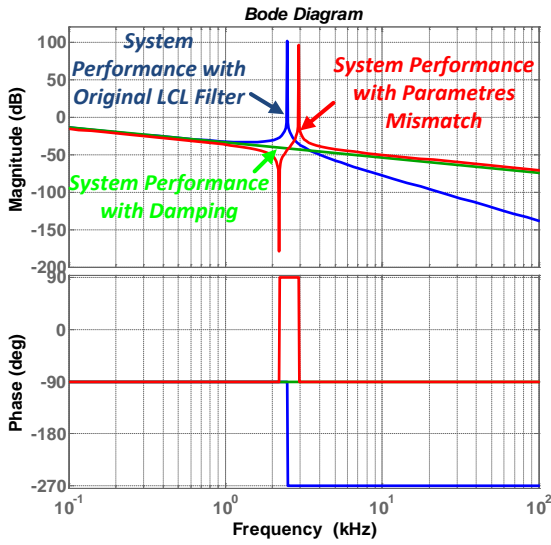
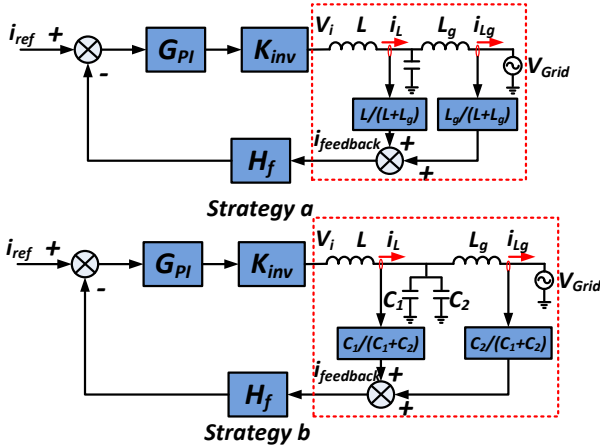
Fig. 5. Bode diagram of L and LCL filter.

Fig. 6. Rectified feedback current control strategy.

A. Feedback Current Rectification

As can be seen in Fig. 5, a single L filter is inherently stable, because the slope is -20dB when magnitude curve crosses 0dB . In [2] and [9], new current feedback strategies are proposed in order to simulate a single L filter behaviour. From the control

diagram illustrated in Fig.6, it can be seen that the feedback current is made up from two components, which depends on L and L_g values or C_1 and C_2 values. By replacing the feedback current with the new ones, loops in red dashed frame will be transformed into an L transfer function without any additional control loop. Thus no resonance peak will be present in the current control loop, as shown in (2).

However, its frequency behaviour still relies on LCL physical features. In fact, this technique represents half of the active damping methods. Inductor and capacitor values in an LCL filter usually change along with their operation time. Once LCL physical parameters are mismatched, the transfer function i_{feedback}/V_i cannot be longer seen as a single L transfer function, and thus more resonance peaks will come out, whose magnitude is nearly as high as the original LCL filter, as shown in Fig. 5. In addition, system cost and complexity will be increased since more current sensors are used in order to obtain the two inductor currents.

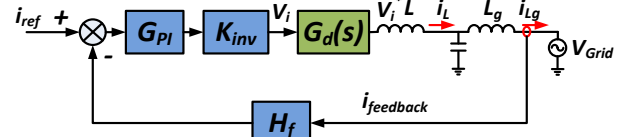


Fig. 7. Block diagram of the control loop.

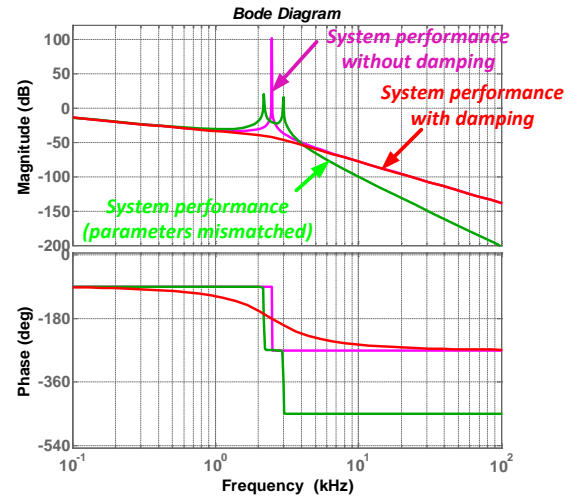


Fig. 8. Bode diagram of the closed-loop system with the control loop rectification.

$$\begin{aligned}
\frac{i_{feedback}}{V_i} &= \frac{L}{L+L_g} \frac{i_L}{V_i} + \frac{L_g}{L+L_g} \frac{i_{L_g}}{V_i} \\
\frac{i_L}{V_i} &= \frac{L_g C s^2}{LL_g C s^3 + (L+L_g)s} \Rightarrow \frac{i_{feedback}}{V_i} = \frac{L}{L+L_g} \frac{L_g C s^2}{LL_g C s^3 + (L+L_g)s} + \frac{L_g}{L+L_g} \frac{1}{LL_g C s^3 + (L+L_g)s} = \frac{1}{(L+L_g)s} \\
\frac{i_{L_g}}{V_i} &= \frac{1}{LL_g C s^3 + (L+L_g)s} \\
\frac{i_{feedback}}{V_i} &= \frac{C_2}{C_1+C_2} \frac{i_L}{V_i} + \frac{C_1}{C_1+C_2} \frac{i_{L_g}}{V_i} \\
\frac{i_L}{V_i} &= \frac{L_g C s^2}{LL_g C s^3 + (L+L_g)s} \Rightarrow \frac{i_{feedback}}{V_i} = \frac{C_2}{C_1+C_2} \frac{L_g C s^2}{LL_g C s^3 + (L+L_g)s} + \frac{C_1}{C_1+C_2} \frac{1}{LL_g C s^3 + (L+L_g)s} = \frac{1}{(L+L_g)s} \\
\frac{i_{L_g}}{V_i} &= \frac{1}{LL_g C s^3 + (L+L_g)s} \\
\frac{L}{L+L_g} &= \frac{C_2}{C_1+C_2}
\end{aligned} \tag{2}$$

B. Auxiliary Filter

In order to remove system dependence on *LCL* filter inherent parameters, filters are chosen as a damp unit, which is inserted into control loops to damp system resonance.

By inserting the filter directly into control loops, inherent unstable elements of the system can be cancelled the (see Fig.7). Based on the transfer function V_i -to- i_c [11], inherent poles in *LCL* transfer function (2) are cancelled in the closed-loop transfer function. As a consequence, the resonance peak in *LCL* filter is effectively damped without affecting filter performance in high-frequency range, having a very similar effect as adding a single damping resistance (*R*) to the *LCL* filter (see Fig.8). The other one is placing filters in the feedback loop, which also aims at eliminating system's instability.

However, this active damping strategy to some extent still depends on *LCL* physical parameters, as shown in (3). The damping term $G_d(s)$ can be deduced from the original transfer function $i_c(s)/V_i(s)$ that contains no damping term. With the aging of the components, both *L* and *C* values will drift, causing a negative effect on the damping performance.

Based on Fig. 8 (see green curve), it can be concluded that performance in high-frequency range is enhanced although two more resonance peaks may appear, which are smaller than that in the original *LCL* filter. However, interaction caused by new resonance peaks may also take place between the grid and the converter, which means that an additional damping block may be still required.

Besides, other types of filters (see Fig. 9), such as notch filter ([26]), lead-lag filter ([10], [14] and [15]) and so on, are also adopted in the feedback loop as a damped element in the system.

C. Virtual Resistors

Although passive damping methods are simpler and cost effective, extra losses always come along thus affecting system efficiency. With capacitor *C* voltage feedback and the proportional gain *K* proposed in [12]-[13], a similar damping function can be realized (see Fig. 10). In (4), a virtual resistor control loop and its transfer function are presented. It can be

seen that it is quite similar to the passive damping methods. Bode diagram shown in Fig. 11 illustrates that the resonance peak is successfully suppressed. Since no real resistors are inserted into the hardware circuit, thus no extra-losses may exist. In this condition, *LCL* parameters mismatch has little effect on the damping method performance. Even in case of *LCL* parameters change or drift, the damping performance is still effective without affecting system performance in high frequency, shown in the red curve of Fig. 10. Notice that only a small position offset of the resonance frequency is caused.

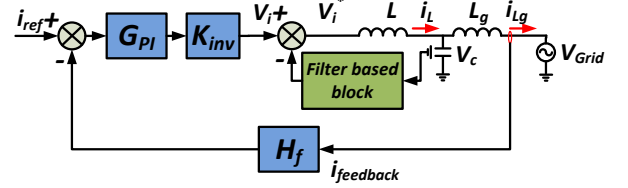


Fig. 9. Lead-lag network control block.

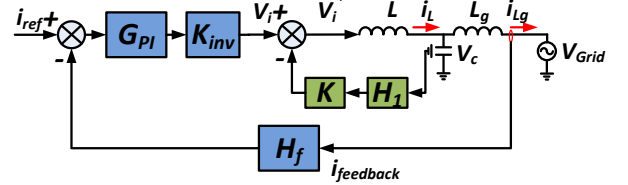


Fig. 10. Block diagram of the virtual resistor loop.

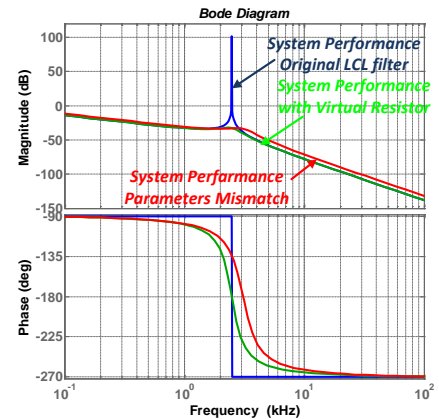


Fig. 11. Bode diagram of the closed-loop system with the virtual resistor loop.

the injected grid-current. Actually, its intrinsic features are the same as capacitor voltage feedback damping, as shown in (6). More poles are placed into the transfer function denominator through the grid current feedback loop. However it only uses one current sensor, which means a lower complexity and cost. However, as aforementioned, this solution is highly dependent on the parameters, so that for instance L_g parameter drift will have a negative effect on damping performance.,

4) *Generalized closed-loop control (GCC)*: Based on virtual resistor damping methods, two damping impedance loops are inserted into the control scheme, including an internal impedance term and an external impedance term, for the sake of both droop control and LCL damping resonance purposes, as shown in Fig.14. This method is intended for microgrid applications. In island mode, converters operate as voltage sources and connected to PCC with the aim of helping droop control. Here, external impedance block regulate converter output impedance in order to enhance system performance and to suppress multiple resonances between multiple LCL -terminated converters [25]. When some converter is required to transfer energy to the grid, the internal impedance loop is used, thus achieving the damping resonance objective. It is to a large extent reliable, but an optimal control strategy is necessary to smooth transfer from island to grid-connected modes.

V. SIMULATION RESULTS

Here some of the damp methods' performances are validated in a 10kW single-phase inverter simulation platform. Simulation results of grid current feedback, inverter output current feedback, weighted current feedback and virtual resistor are shown from Fig.15 to Fig. 18.

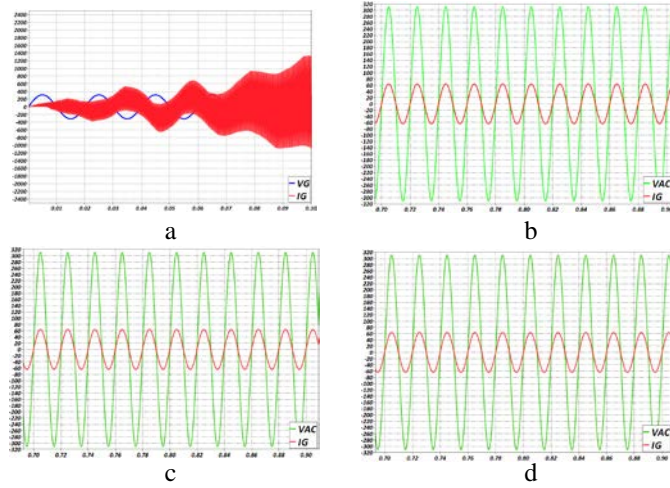


Fig.15. Voltage and current under different damp method (a: only grid current feedback, b: only inverter output current feedback, c: weighted current feedback d: virtual resistor).

When only grid current is feedback, the system is unstable (see Fig.15 (a)). With the other three control strategies, grid injected current is smooth and stable (see Fig. 15 b to d).

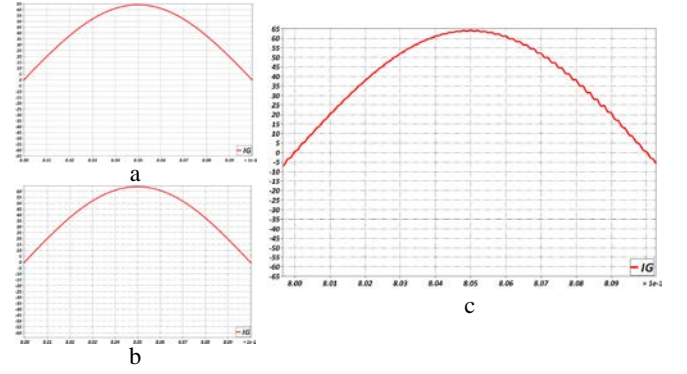


Fig.16. Current with inverter output current feedback (a: normal condition, b: L_g 's value is changed by 10%, c: L 's value is changed by 10%).

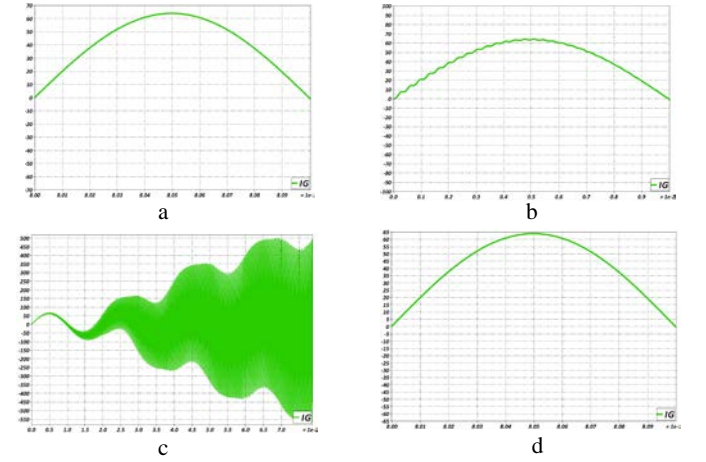


Fig.17. Current with weighted current feedback (a: normal condition, b: start process when L 's value is changed by 10%, c: L_g 's value is changed by 10%, d: L 's value is changed by 10%).

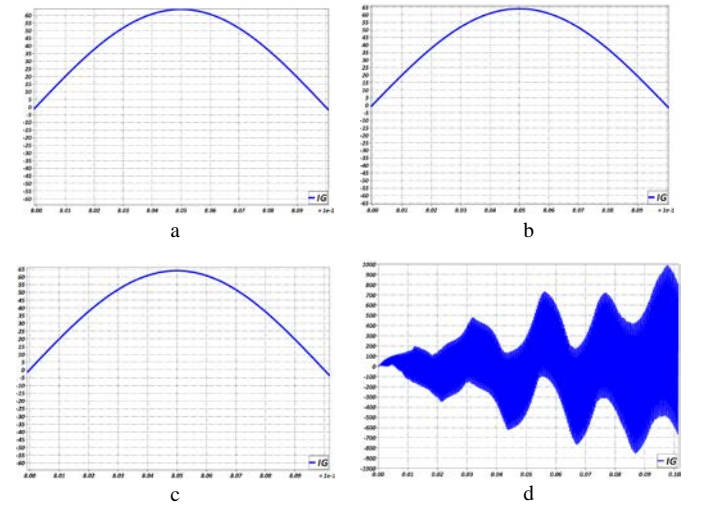


Fig.18. Current with virtual resistor (a: normal condition, b: L 's value is reduced by 10%, c: L_g 's value is changed by 10%, d: bigger virtual resistor).

In order to validate different control strategies' performance when LCL 's physical parameters are drifted, more simulations were carried out (see from Fig. 16 to Fig. 17).

When changing L_g 's value by 10%, grid current of the inverter is affected if only the converter output current is feedback (see Fig. 16 (a) and (b)). However, there are some high frequency resonances in grid current if L 's value is changed by 10% (see Fig.16 (c)).

In Fig. 17, results under different conditions are shown when weighted current feedback is adopted. When L 's value is changed, there exist some other frequency resonances in grid injected current (see Fig. 17 (b)). Nevertheless, it can be also suppressed successfully gradually (see Fig. 17 (d)). If L_g 's value is reduced by 10%, system is divergent. Consequently, weighted current feedback is sensitive to LCL 's physical parameters' mismatch, especially L_g .

At the same time, virtual resistor is less sensitive to LCL 's physical parameters (see Fig. 18). No matter how the parameters are changed, grid current is clean and stable (see Fig. 18 (a) (b) and (c)). But there is limitation on virtual resistor's value. Once an improper value is given, grid current will be divergent (see Fig. 18 (d)).

VI. CONCLUSION

LCL filter becomes more and more used in practical applications since its good performance in attenuating harmonics injected into grid and its contribution in minimizing filter size. However, LCL filter impedance is zero at its resonance frequency, so that a resonance peak will cause oscillation in the control loop. In order to suppress resonance brought by the LCL filter, active, passive, hybrid, and other improved methods are proposed in order to enhance system performance in both low and high frequency ranges. An optimal balance between circuits' losses (in passive methods) and system complexity (in active methods) should be made carefully. When designing the control strategy for an LCL interface grid-connected converters, the following rules should be followed:

- Lower circuit losses
- Lower system complexity
- Reduce AD sensors (Current sensors) and system cost
- Enhance reliability and accuracy

In applications such as microgrids, every converter will work as a current source to inject current to the grid, and L , C and L_{droop} can be treated as a LCL filter. Resonance may exist since many LCL filters are connected to the PCC at the same time. So that with an optimal control strategy aiming at LCL filter, better performance in both stable and transient performance can be achieved.

This paper analysis is mainly focused in frequency domain. So in the future works more emphasis should be put in discrete domain to get more accurate results, including sample and hold, control delays, and more simulation will be carried out to evaluate different damping method.

REFERENCES

- [1] Liserre, M.; Blaabjerg, F.; Hansen, S., "Design and control of an LCL-filter based three-phase active rectifier," *Industry Applications Conference, 2001. Thirty-Sixth IAS Annual Meeting. Conference Record of the 2001 IEEE*, vol.1, no., pp.299,307 vol.1, Sept. 30 2001-Oct.4 2001
- [2] Guoqiao Shen; Xuancai Zhu; Min Chen; Dehong Xu, "A New Current Feedback PR Control Strategy for Grid-Connected VSI with an LCL Filter," *Applied Power Electronics Conference and Exposition, 2009. APEC 2009. Twenty-Fourth Annual IEEE*, vol., no., pp.1564,1569, 15-19 Feb. 2009
- [3] Weimin Wu; Yuanbin He; Tianhao Tang; Blaabjerg, F., "A New Design Method for the Passive Damped LCL and LLCL Filter-Based Single-Phase Grid-Tied Inverter," *Industrial Electronics, IEEE Transactions on*, vol.60, no.10, pp.4339,4350, Oct. 2013
- [4] Dahono, P.A., "A control method to damp oscillation in the input LC Filter," *Power Electronics Specialists Conference, 2002. pesc 02. 2002 IEEE 33rd Annual*, vol.4, no., pp.1630,1635, 2002
- [5] Wang, T.C.Y.; Zhihong Ye; Gautam Sinha; Xiaoming Yuan, "Output filter design for a grid-interconnected three-phase inverter," *Power Electronics Specialists Conference, 2003. PESC '03. 2003 IEEE 34th Annual*, vol.2, no., pp.779,784 vol.2, 15-19 June 2003
- [6] Channegowda, P.; John, V., "Filter Optimization for Grid Interactive Voltage Source Inverters," *Industrial Electronics, IEEE Transactions on*, vol.57, no.12, pp.4106,4114, Dec. 2010
- [7] Turner, R.; Walton, S.; Duke, R., "Stability and Bandwidth Implications of Digitally Controlled Grid-Connected Parallel Inverters," *Industrial Electronics, IEEE Transactions on*, vol.57, no.11, pp.3685,3694, Nov. 2010
- [8] Rockhill, A.A.; Liserre, M.; Teodorescu, R.; Rodriguez, P., "Grid-Filter Design for a Multimegawatt Medium-Voltage Voltage-Source Inverter," *Industrial Electronics, IEEE Transactions on*, vol.58, no.4, pp.1205,1217, April 2011
- [9] Guoqiao Shen; Dehong Xu; Luping Cao; Xuancai Zhu, "An Improved Control Strategy for Grid-Connected Voltage Source Inverters With an LCL Filter," *Power Electronics, IEEE Transactions on*, vol.23, no.4, pp.1899,1906, July 2008
- [10] Liserre, M.; Dell'Aquila, A.; Blaabjerg, F., "Stability improvements of an LCL-filter based three-phase active rectifier," *Power Electronics Specialists Conference, 2002. pesc 02. 2002 IEEE 33rd Annual*, vol.3, no., pp.1195,1201 vol.3, 2002
- [11] Chuan Xie; Yue Wang; Xiaojian Zhong; Guozhu Chen, "A novel active damping method for LCL-filter-based shunt Active Power Filter," *Industrial Electronics (ISIE), 2012 IEEE International Symposium on*, vol., no., pp.64,69, 28-31 May 2012
- [12] Gullvik, W.; Norum, L.; Nilsen, R., "Active damping of resonance oscillations in LCL-filters based on virtual flux and virtual resistor," *Power Electronics and Applications, 2007 European Conference on*, vol., no., pp.1,10, 2-5 Sept. 2007
- [13] Wessels, C.; Dannehl, J.; Fuchs, F.W., "Active damping of LCL-filter resonance based on virtual resistor for PWM rectifiers — stability analysis with different filter parameters," *Power Electronics Specialists Conference, 2008. PESC 2008. IEEE*, vol., no., pp.3532,3538, 15-19 June 2008
- [14] Pena-Alzola, R.; Liserre, M.; Blaabjerg, F.; Sebastian, R.; Dannehl, J.; Fuchs, F.W., "Systematic Design of the Lead-Lag Network Method for Active Damping in LCL-Filter Based Three Phase Converters," *Industrial Informatics, IEEE Transactions on*, vol.10, no.1, pp.43,52, Feb. 2014
- [15] Ricchiuto, D.; Liserre, M.; Kerekas, T.; Teodorescu, R.; Blaabjerg, F., "Robustness analysis of active damping methods for an inverter connected to the grid with an LCL-filter," *Energy Conversion Congress and Exposition (ECCE), 2011 IEEE*, vol., no., pp.2028,2035, 17-22 Sept. 2011
- [16] Peña-Alzola, R.; Liserre, M.; Blaabjerg, F.; Sebastián, R.; Dannehl, J.; Fuchs, F.W., "Analysis of the Passive Damping Losses in LCL-Filter-Based Grid Converters," *Power Electronics, IEEE Transactions on*, vol.28, no.6, pp.2642,2646, June 2013
- [17] Dannehl, J.; Fuchs, F.W.; Hansen, S.; Thøgersen, P.B., "Investigation of Active Damping Approaches for PI-Based Current Control of Grid-Connected Pulse Width Modulation Converters With LCL

-
- Filters," *Industry Applications, IEEE Transactions on*, vol.46, no.4, pp.1509,1517, July-Aug. 2010
- [18] Mukherjee, N.; De, D., "Analysis and improvement of performance in LCL filter-based PWM rectifier/inverter application using hybrid damping approach," *Power Electronics, IET*, vol.6, no.2, pp.309,325, Feb. 2013
- [19] Liserre, M.; Aquila, A.D.; Blaabjerg, F., "Genetic algorithm-based design of the active damping for an LCL-filter three-phase active rectifier," *Power Electronics, IEEE Transactions on*, vol.19, no.1, pp.76,86, Jan. 2004
- [20] Xu, J.; Xie, S.; Tang, T., "Active Damping-Based Control for Grid-Connected LCL-Filtered Inverter With Injected Grid Current Feedback Only," *Industrial Electronics, IEEE Transactions on*, vol.61, no.9, pp.4746,4758, Sept. 2014
- [21] Jinwei He; Yun Wei Li, "Generalized Closed-Loop Control Schemes with Embedded Virtual Impedances for Voltage Source Converters with LC or LCL Filters," *Power Electronics, IEEE Transactions on*, vol.27, no.4, pp.1850,1861, April 2012
- [22] Guerrero, J.M.; Garcia de Vicuna, L.; Matas, J.; Castilla, M.; Miret, J., "A wireless controller to enhance dynamic performance of parallel inverters in distributed generation systems," *Power Electronics, IEEE Transactions on*, vol.19, no.5, pp.1205,1213, Sept. 2004
- [23] Guerrero, J.M.; Chandorkar, M.; Lee, T.; Loh, P.C., "Advanced Control Architectures for Intelligent Microgrids—Part I: Decentralized and Hierarchical Control," *Industrial Electronics, IEEE Transactions on*, vol.60, no.4, pp.1254,1262, April 2013
- [24] D. Goldberg, *Genetic Algorithms in Optimization and Machine Learning*. Reading, MA: Addison-Wesley, 1989.
- [25] Jinwei He; Yun Wei Li; Bosnjak, D.; Harris, B., "Investigation and Active Damping of Multiple Resonances in a Parallel-Inverter-Based Microgrid," *Power Electronics, IEEE Transactions on*, vol.28, no.1, pp.234,246, Jan. 2013
- [26] Dannehl, J.; Liserre, M.; Fuchs, F.W., "Filter-Based Active Damping of Voltage Source Converters With LCL Filter," *Industrial Electronics, IEEE Transactions on*, vol.58, no.8, pp.3623,3633, Aug. 2011